

## Electro-oxidation of organic fuels catalyzed by ultrasmall silicon nanoparticles

Yongki Choi,<sup>1,a)</sup> Gang Wang,<sup>1</sup> Munir H. Nayfeh,<sup>2,b)</sup> and Siu-Tung Yau<sup>1,3,b)</sup>

<sup>1</sup>Department of Electrical and Computer Engineering, Cleveland State University, Cleveland, Ohio 44115, USA

<sup>2</sup>Department of Physics, University of Illinois at Urbana-Champaign, Urbana, Illinois 61801, USA

<sup>3</sup>Applied Biomedical Engineering, Cleveland State University, Cleveland, Ohio 44115, USA

(Received 16 September 2008; accepted 22 September 2008; published online 22 October 2008)

Ultrasmall colloidal silicon nanoparticles behave as electrocatalysts for the oxidation of ethanol, methanol, and glucose. Electrochemical characterization of particle-immobilized electrodes shows a catalytic onset between  $-0.4$  and  $0$  V versus Ag/AgCl at neutral pH. The onset potential and the catalytic strength are dependent on the particle size. A prototype hybrid biofuel cell was constructed, using the particles as the anode catalyst. The catalytic activity undergoes a 50-fold increase under alkaline condition compared to that under acidic condition. An unexpected light dependence of the catalytic current was observed. A significant increase in the catalytic current is obtained when the catalysis is performed in darkness. © 2008 American Institute of Physics.

[DOI: 10.1063/1.3001594]

To utilize renewable energy resources such as organic fuels, new electrocatalysts, especially those with novel properties due to their nanoscale characteristic dimensions, need to be discovered for energy-harvesting applications.<sup>1</sup> Presently, the platinum-ruthenium (Pt–Ru) alloy system is used as the anode catalyst in direct alcohol fuel cells<sup>2</sup> for high-power applications. Precious-metal catalysts are expensive and their supply is limited.<sup>3</sup> For low-power applications such as nanodevices,<sup>4</sup> power levels ranging from nanowatts to microwatts are required for device operation. An important application for low-power generation is implantable power supply,<sup>5</sup> where the enzyme-based biofuel cell is envisaged to use a physiologically ambient glucose as fuel to power implanted biomedical devices such as cardiac pacemakers<sup>6</sup> and artificial hearing devices.<sup>7</sup> A typical power level of  $\sim 1$   $\mu$ W is required for the operation of the cardiac pacemaker.<sup>8</sup> However, enzymes' inherent instability makes biofuel cells' long-term performance unstable.<sup>5</sup>

Here, we show that ultrasmall colloidal silicon nanoparticles behave as electrocatalysts for the electro-oxidation of ethanol, methanol, and glucose. Electrochemical characterization shows that the catalytic onset occurs between  $-0.4$  and  $0$  V versus Ag/AgCl at neutral pH. The onset and catalytic strength are dependent on particle size. A prototype hybrid fuel cell was constructed, using the particles as the anode catalyst, to demonstrate the potentiality of the particles in low-power generation. The catalytic activity undergoes a 50-fold increase under alkaline condition compared to that under acidic condition. An intriguing feature of the particle-induced catalysis is an unexpected light dependence that a significant increase in the catalytic current is obtained when the catalysis is performed in darkness.

The silicon nanoparticles were made by electrochemical etching of a *p*-type silicon wafer in hydrofluoric acid and hydrogen peroxide followed by ultrasonically shaking off the

particles from the wafer in a solvent to form a colloid.<sup>9</sup> This technique can be used to prepare 1 nm particles (Si1) and 2.8 nm particles (Si2.8). *n*-type heavily doped ( $\rho < 0.005$   $\Omega$  cm) silicon wafers were used as electrodes to support the particles. The preparation of the particle-immobilized silicon electrode was described previously.<sup>10</sup> Atomic force microscopy of the electrode surface showed the presence of the particles at a submonolayer level.<sup>10</sup> Two types of silicon electrodes were made: silicon wafers immobilized with the Si1 particle (the Si1–Si electrode) and those immobilized with the Si2.8 particle (the Si2.8–Si electrode). Carbon paper (Toray, TGPH-120) was also used as electrode for its porosity, which leads to improved particle loading. The particle-immobilized carbon paper electrodes (the Si1–CP electrode and the Si2.8–CP electrode) have a particle surface density of 28  $\mu$ g/cm<sup>2</sup>. Voltammetry measurements were made with a typical three-electrode electrochemical cell. A commercial Ag/AgCl (3M KCl) electrode was used as the reference electrode, and a platinum wire was used as the counterelectrode. Purified water ( $\rho = 18.2$  M $\Omega$  cm) was used to prepare 100 mM phosphate buffer solution (PBS). The fuels [ $\beta$ -D(+)-glucose from Sigma, 99.9% methanol and 99.5% ethanol from ACROS] were dissolved in PBS. Cyclic voltammograms (CVs) and linear sweep voltammograms (LSVs) were obtained at 50 mV/s. Tafel measurement was performed at 1 mV/s. Control experiments performed with bare working electrodes showed no electrochemical response to the fuels up to a potential as high as 1.6 V. Highly oriented pyrolytic graphite (HOPG) was also used as fuel cell electrodes. All measurements were made at room temperature.

The electrochemical responses of the particle-immobilized electrodes to ethanol, methanol, and glucose have been studied. The CVs of a Si1–Si electrode and a Si2.8–Si electrode obtained in ethanol are shown in Fig. 1(a). The black CV is the electrodes' background signal obtained in PBS at pH 7. The blue CV and the red CV were obtained with the Si1–Si electrode and the Si2.8–Si electrode, respectively, in 20 mM ethanol dissolved in the PBS. The increases in the anodic currents of the blue and red CVs above the background start at  $-0.4$  and  $0$  V versus Ag/AgCl, respec-

<sup>a)</sup>Also at Department of Physics, Graduate Center of City University of New York, New York, NY 10016-4309.

<sup>b)</sup>Authors to whom correspondence should be addressed. Electronic addresses: m-nayfeh@uiuc.edu and s.yau@csuohio.edu.

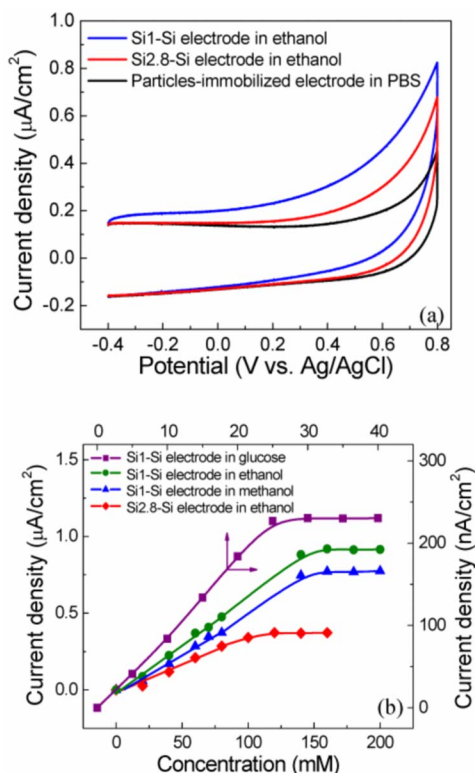


FIG. 1. (Color online) Electrochemical characterization of the particle-immobilized silicon electrodes in ethanol, methanol, and glucose. (a) CVs of a Si1-Si electrode and a Si2.8-Si electrode in PBS (the background) at pH 7 and in the same PBS containing 20 mM ethanol. (b) The ethanol calibration curves of the same electrodes as in (a) and the calibration curves of the Si1-Si electrode for methanol and glucose at pH 7. The ethanol calibration curves were obtained at potentials of 0.2 and 0.3 V for the Si1-Si electrode and the Si2.8-Si electrode, respectively. The methanol and glucose calibration curves were obtained at 0.2 V. Each data point shows the fuel oxidation current obtained by subtracting the background current from the total anodic current. Similar calibration results were obtained with different electrodes.

tively. The bare silicon wafer shows no such response to ethanol. Thus, the particles exhibit a catalytic character in the electro-oxidation of ethanol. The electrodes' ethanol calibration curves in Fig. 1(b) indicate that the Si1 particle, compared to the Si2.8 particle, generates a greater amount of current. Thus, both the onset potential and the strength of the catalysis depend on the particle size. The electrochemical responses of the two types of electrodes to methanol and glucose show similar catalytic characteristics. The calibration curves of the Si1-Si electrode for methanol and glucose are shown in Fig. 1(b). Similar electrochemical responses to the three fuels were also observed with particle-loaded CP electrodes.

Tafel plots (curves not shown) of the electrodes were obtained at pH 7. Table I shows the Tafel slopes for a Si2.8-Si electrode in the fuels. The Tafel slope yields the value of the product  $an$ ,  $\alpha$  being the electron transfer coef-

TABLE I. Kinetic parameters of the catalytic processes of the three fuels using the Si2.8-Si electrode.

	Tafel slope (mV/decade)	$an$	$n$	Reaction order
Methanol	178	0.33	1	1.29
Ethanol	212	0.28	1	1.03
Glucose	180	0.33	1	1.07

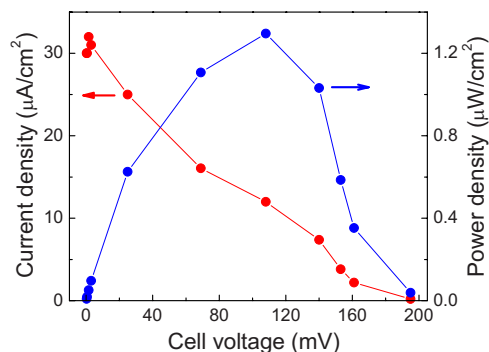


FIG. 2. (Color online) The  $I$ - $V$  and  $P$ - $V$  characteristics of the prototype hybrid biofuel cell in 200 mM glucose at room temperature and pH 7. The particle-immobilized HOPG anode and the enzyme-immobilized HOPG cathode were put inside a 30 ml beaker which contained glucose dissolved in PBS.

ficient and  $n$  the number of electrons transferred in the reaction.<sup>11</sup> The values of  $an$  for the three reactions suggest  $n=1$  from Table I, which also shows the orders of the reactions. Therefore, the electro-oxidation of the fuels appears to be a first order reaction with  $n=1$ .

We have constructed a prototype single-compartment hybrid fuel cell that operates on glucose. Si1 particles were used as the anode catalyst for the electro-oxidation of glucose to produce electrons, which generate a current in the external circuit. Two enzymes, microperoxidase (MP-11) and glucose oxidase (GOx), were coimmobilized on the cathode.<sup>12</sup> GOx catalyzed the oxidation of glucose to produce  $H_2O_2$ , which diffused to MP-11 to be reduced to water. Figure 2 shows the cell current versus cell voltage ( $I$ - $V$ ) and the power density versus cell voltage ( $P$ - $V$ ) characteristics of the fuel cell. At 200 mM glucose, the cell's open-circuit voltage is 0.20 V and the peak power density is  $1.3 \mu W cm^{-2}$ . The  $I$ - $V$  characteristic shows a deviation from the ideal rectangular shape. This deviation could be a result of mass transport losses, reducing the cell voltage below its reversible thermodynamic value.<sup>13</sup> The power output of the fuel cell can be improved by employing a more efficient cathode reaction such as the reduction of oxygen to water using bilirubin oxidase.<sup>14</sup>

Electro-oxidation of ethanol and methanol on the Pt electrode proceeds by adsorption of fuel fragments on the electrode.<sup>15</sup> The double-peak hysteresis structure observed in the CV is caused by electrode poisoning due to adsorption of CO and subsequent oxidation of the Pt electrode.<sup>16</sup> The oxidation starts at a high potential of 0.5 V versus RHE.<sup>16,17</sup> The bifunctional Pt-Ru system lowers the oxidation onset to  $\sim 0.4$  V versus RHE by removing CO with oxygen-containing adsorbates such as OH.<sup>18</sup> The activities of Pt and Pt-Ru for these fuels are stronger under alkaline condition than under acid condition.<sup>17</sup>

The particle-catalyzed oxidation of the fuels result in a monotonous increase in the anodic current with an onset, suggesting a direct catalysis pathway.<sup>19</sup> The onset for ethanol and methanol between  $-0.4$  and  $0$  V versus Ag/AgCl (or  $-0.62$  and  $-0.22$  V versus RHE). Figure 3 shows the LSVs of the Si1 particle in ethanol under acidic, neutral, and alkaline conditions. The particle shows a significantly larger activity under alkaline condition than under acidic condition. At low potentials the activity shows a 50-fold increase under alkaline condition. Therefore, the pH dependence of the cata-

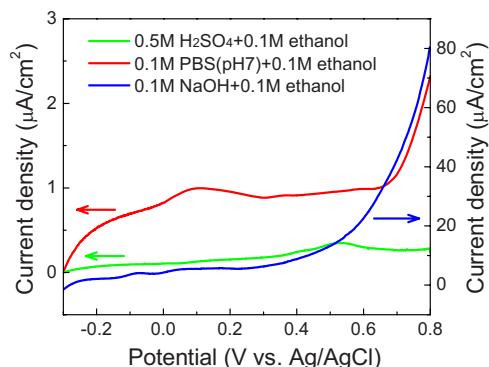


FIG. 3. (Color online) The pH dependence of the particle-catalyzed electro-oxidation of ethanol. The LSVs were obtained with a Si1-CP electrode. Each LSV shows the fuel oxidation current obtained by subtracting the background current from the total anodic current.

lytic activity of the silicon particles is qualitatively similar to those of Pt and Pt–Ru. The pH dependence for the Pt/Pt–Ru systems is attributed to the pH competitive adsorption of oxygenated species with anions from supporting electrolytes,<sup>20</sup> while the cause is not clear yet in the present study.

In this study, an unexpected light-dependent phenomenon was observed. The catalytic currents of the three fuels show a substantial and persistent increase when the catalysis is performed in darkness as compared to performing the same experiment in light. Figure 4(a) shows the CVs ob-

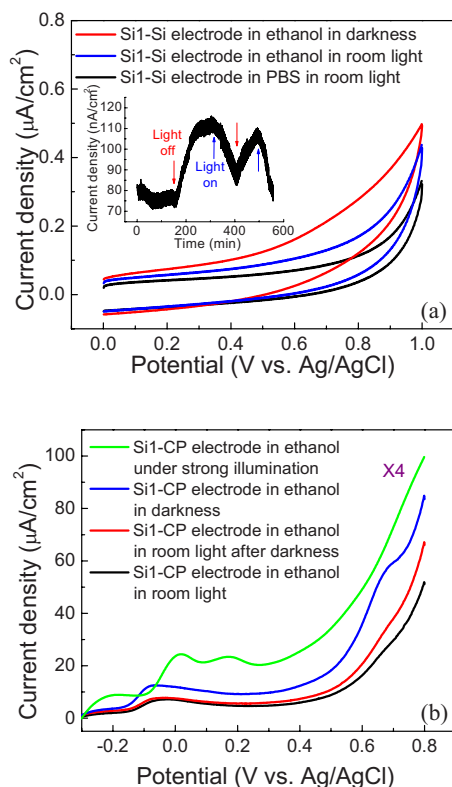


FIG. 4. (Color online) The effect of white light illumination and darkness on ethanol oxidation current. (a) The current density produced by a Si1–Si electrode in 200 mM ethanol at pH 7 shows an increase in darkness as compared to that produced in room light (0.5 mW/cm<sup>2</sup>). The inset is a current-time trace, showing the effect of turning off and turning on the light. The trace was obtained using a different electrode at 0.3 V and 200 mM of ethanol. (b) The catalytic current produced by a Si1-CP electrode in 200 mM ethanol at pH 13 in room light, in darkness, and under strong illumination of 200 mW/cm<sup>2</sup> at pH 13.

tained in an ethanol experiment with a Si1–Si electrode in room light (white fluorescent light with an intensity of 0.5 mW/cm<sup>2</sup>) and darkness at pH 7. Darkness caused the oxidation current to increase above the room-light oxidation current. The minimum of this increase is more than twofold as shown in Fig. 4(a). The inset of Fig. 4(a) shows this effect in a time trace using a different Si1–Si electrode. Turning off the light caused an increase of 35 nA/cm<sup>2</sup> in the oxidation current density above that observed in the light. Figure 4(b) shows this light-dependent effect observed with a Si1-CP electrode in ethanol at pH 13.

To emphasize this unusual light-dependent phenomenon, we have performed the catalysis under strong illumination. Figure 4(b) shows that reilluminating the electrode with room light brings the current almost back to the original room-light value. However, when the electrode is illuminated with white light with intensity of 200 mW/cm<sup>2</sup>, the oxidation current shows a 14-fold increase in the current as compared to the room-light current. The increased catalytic current caused by light is conceptually expected since the heat generated in the system by light can be used as energy to overcome the activation barrier to enhance the reaction rate. However, low-intensity light may excite excitons across the 3 eV band gap of the Si1 particle<sup>21</sup> with a long recombination lifetime, a characteristic of the particles.<sup>22</sup> The excitons may block the conduction of electrons from the ionized molecules and hence diminishes the oxidation current.

S.-T.Y. acknowledges the support from Cleveland State University.

<sup>1</sup>D. R. Rolison, *Science* **299**, 1698 (2003).

<sup>2</sup>*Handbook of Fuel Cells—Fundamentals, Technology and Applications*, edited by W. Vielstich, H. A. Gasteiger, and A. Lamm (Wiley, New York, 2003), Vol. 2.

<sup>3</sup>S. G. Chalk and J. F. Miller, *J. Power Sources* **159**, 73 (2006).

<sup>4</sup>A. Bachtold, P. Hadley, T. Nakanishi, and C. Dekker, *Science* **294**, 1317 (2001).

<sup>5</sup>S. C. Barton, J. Gallaway, and P. Atanassov, *Chem. Rev. (Washington, D.C.)* **104**, 4867 (2004).

<sup>6</sup>C. F. Holmes, *Electrochem. Soc. Interface* **12**, 26 (2003).

<sup>7</sup>J. P. Rauschecker and R. V. Shannon, *Science* **295**, 1025 (2002).

<sup>8</sup>D. Linden and T. B. Reddy, *Handbook of Batteries*, 3rd ed. (McGraw-Hill, New York, 2002).

<sup>9</sup>G. Belomoin, J. Therrien, and M. Nayfeh, *Appl. Phys. Lett.* **77**, 779 (2000).

<sup>10</sup>G. Wang, K. Mantey, M. H. Nayfeh, and S.-T. Yau, *Appl. Phys. Lett.* **89**, 243901 (2006).

<sup>11</sup>A. J. Bard and L. R. Faulkner, *Electrochemical Methods*, 2nd ed. (Wiley, Hoboken, NJ, 2001).

<sup>12</sup>A. Ramanavicius, A. Kausaite, and A. Ramanavicius, *Biosens. Bioelectron.* **20**, 1962 (2005).

<sup>13</sup>A. Habrioux, E. Sibert, K. Servat, W. Vogel, K. B. Kokoh, and N. Alonso-Vante, *J. Phys. Chem. B* **111**, 10329 (2007).

<sup>14</sup>N. Mano, F. Mao, and A. Heller, *J. Am. Chem. Soc.* **124**, 12962 (2002).

<sup>15</sup>T. Iwasita, in *Handbook of Fuel Cells—Fundamentals, Technology and Applications*, edited by W. Vielstich, H. A. Gasteiger, and A. Lamm (Wiley, New York, 2003), Vol. 2, pp. 603–624.

<sup>16</sup>J. L. Cohen, D. J. Volpe, and H. D. Abruna, *Phys. Chem. Chem. Phys.* **9**, 49 (2007).

<sup>17</sup>H. Wang, Z. Jusys, and R. J. Behm, *J. Phys. Chem. B* **108**, 19413 (2004).

<sup>18</sup>Z. Jusys, J. Kaiser, and R. J. Behm, *Electrochim. Acta* **47**, 3693 (2002).

<sup>19</sup>S. Trasatti, in *Interfacial Electrochemistry: Theory, Experiment and Applications*, edited by A. Wieckowski (Dekker, New York, 1999), pp. 769–792.

<sup>20</sup>A. V. Tripkovic, K. D. Popovic, B. N. Grgur, B. Blizanac, P. N. Ross, and N. M. Markovic, *Electrochim. Acta* **47**, 3707 (2002).

<sup>21</sup>S. Rao, J. Sutin, R. Clegg, E. Gratton, M. H. Nayfeh, S. Habbal, A. Tsolakidis, and R. M. Martin, *Phys. Rev. B* **69**, 205319 (2004).

<sup>22</sup>J. Therrien, Ph.D. thesis, University of Illinois, 2002.